

Smarticle 2.0: Design of Scalable, Entangled Smart Matter

Danna Ma¹, Jiahe Chen¹, Sadie Cutler², Kirstin Petersen¹

¹ School of Electrical and Computer Engineering, Cornell University, Ithaca, NY 14853, USA,

{dm797, jc3472, kirstin}@cornell.edu

² Sibley School of Mechanical and Aerospace Engineering, Cornell University, Ithaca, NY 14853, USA, {sc3236}@cornell.edu

Abstract. We present a new iteration of smart active matter modules capable of unprecedented 3D entanglement, designed specifically for fabrication and operation at large scales by a range of scientific users. We discuss the benefits of entanglement compared to traditional rigid, lattice formations in active matter and modular robots, and the design which supports low cost, a small and appropriate form factor, low weight, low barrier-of-entry, and ease of operation. We characterize the platform in terms of actuation repeatability and longevity, lifting and holding strength, a number of sensing modalities, and battery life. We demonstrate short and (relatively) long range communication using tactile and acoustic transceivers. We further show exploratory collective behaviors with up to 10 modules, including static entanglement and self disassembly. We hope that this open-source ‘robo-physical’ platform can pave the way for new innovations across the fields of modular robots and active and soft matter.

Keywords: scalable collective, modular robot, active matter

1 Introduction

Smart robotic matter consists of large aggregates of programmable units capable of actuation, sensing, and intelligent response to their surroundings [1]. It promises applications both as a physical test platform to gather further insights on materials, colloids, and biological swarms [2, 3], as well as, the ability to act as a taskable, modular robot that can morph between shapes and change properties as needed [4–6]. Demonstrations currently span swarms of carefully linked, individually-capable modules [1, 5], to loose aggregates of modules with little-to-no individual mobility, sensing, or computation [2, 7, 8]. The latter is of special interest in this article because system-wide complexity and functionality can emerge from local interactions between large numbers of individually limited components. However, it also involves significant challenges related to scalable fabrication and operation, and methods for coordination and reliable autonomy.

This paper presents the newest iteration of a Smarticle (smart active matter) robot platform [2], specifically designed to support affordable and large-scale

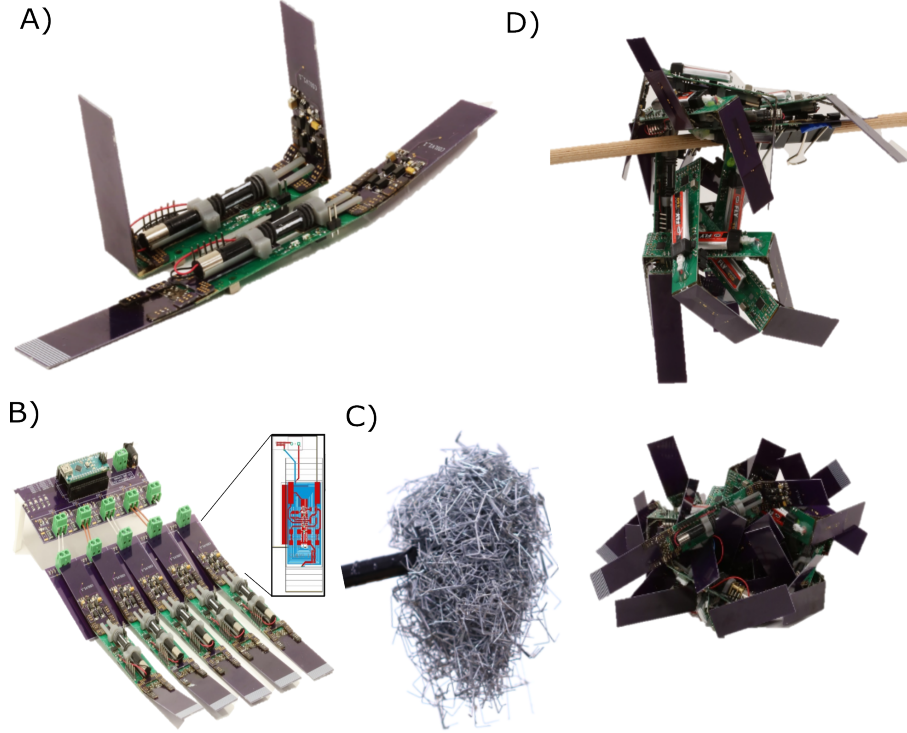


Fig. 1. A) Smarticle 2.0 modules, capable of transitioning between “I” and “U” shapes. B) Wireless charging circuit. C) Entangled staples hanging from a ruler. D) 20 entangled modules.

operation, 3D entanglement, a variety of sensing modalities, and low barrier of entry for novice users across scientific fields (Fig. 1). A Smarticle 2.0 module has a long slender profile that can alternate between a staple-like shape (“U”) and an oblong shape (“I”) using a single actuator, and has the ability to sense and communicate acoustically, optically, and mechanically.

This article focuses on the details of the Smarticle 2.0 design (Sec. 3), fabrication (Sec. 4), and mechanical and sensor characterization (Sec. 5). However, we also show some exploratory multi-robot experiments with up to 10 robots (Sec. 6). To clarify the results presented, we recommend that the reader watches the accompanying video (<https://youtu.be/KrcyYz2ccdg>). To the best of our knowledge, this is the first demonstration of a smart matter platform capable of large-scale, 3D entangled operation.

2 Background and Related Work

The typical trend in smart matter is to rely on modules with sufficient locomotion, sensing, communication, and reasoning skills to function on their own or in small numbers [5, 1]. However, more recent works have suggested that smart matter can be composed of much less capable modules that are largely agnostic

to each other and their surroundings. Examples include modules that are individually immobile, but collectively move [9–11], and, perhaps more impressively, exhibit emergent intelligent behaviors in loose aggregates with only very coarse perception and no explicit communication [10, 12, 8, 13].

One of the major practical issues with smart matter and modular robots is the design of couplings/connection points. Beyond supporting the weight of adjoining modules, these connection points are often used to transfer drive forces, communication signals, and power. In reconfigurable robotic matter, these mechanisms must dock and undock repeatedly and with high accuracy. Hence, these coupling mechanisms are often responsible for a significant fraction of the weight, volume, price, and wear. To overcome this issue, many platforms rely on active or passive magnetic coupling [5, 14, 1], with the explicit trade-off of low force transfer which limits configurations to small overhangs or planar operation. Another interesting tangent are modules with compliant magnetic couplings, which permit loosely coupled aggregates in non-lattice formations [8–10]. A final promising option is the reversible fusion of surface material, as demonstrated in 3D modular robots [15].

The Smarticles, first presented in 2015 [2], breaks with these discrete on/off unit couplings by leveraging entanglement of convex modules. Entanglement is advantageous because 1) it does not require precise module-module alignment; 2) it does not require expensive, heavy, and bulky coupling mechanisms; and 3) although it cannot produce particular formations, it permits modules to couple loosely to generate materials and conglomerates with different shapes and rheological and structural properties like viscosity, yield stress, and packing density. The Smarticles entangle simply by leveraging two rotating appendages, causing units to alternate between “U”, “I”, and, in some cases, “Z” shapes. In spite of their simplicity, Smarticle aggregates have been shown to move collectively when many are confined in a small space [11], and to perform phototaxis using only binary sensor inputs and physical interactions [16, 12]. Further demonstrating their versatility, they have also been used for physics studies, e.g. pertaining to non-equilibrium ordering phenomena [3] and novel phase dynamics in active matter [17] and biological model systems [18].

While the original inspiration for the Smarticles platform stems from 3D entanglement of “U”-shaped particles [19], all prior demonstrations have been restricted to planar operation. The reason is two-fold. Most importantly, the Smarticle 1.0 prototype does not have a profile that supports effective 3D entanglement. Each module can only entangle with one other due to the aspect ratio. Furthermore, the current prototype was not optimized for operation in large robot swarms which are needed for the stochastic effects to average out. In this paper, we present a new design which enables full 3D entanglement, large scale deployment, and may serve as an easily accessible platform to support novel studies on smart and active matter systems.

3 Electro-Mechanical Design

Compared to other modular and swarming robots in literature (Table 1), the Smarticles 2.0 have a relatively small form factor ($2000 \times 20 \times 17\text{mm}^3$), very light

weight (20g), low cost (< 71USD/pcs) and assembly time ($\sim 15\text{min}$), making it feasible to acquire and operate many in traditional research labs (Table 1). Equally important, the modules have an optimal aspect ratio which is the key to 3D entanglement ($l/w = 0.4 - 0.75$ [19]). Smarticle 2.0 can translate between “I” and “U” shapes leveraging a non-backdrivable 4-bar crank and slider mechanism. Modules also have the ability to sense and communicate optically, acoustically, and mechanically. Finally, modules are powered by a Venom Fly 180mAh 3.7V Lithium Polymer battery which can support reasonably long experiments (up to 200 appendage cycles).

The cost of a module breaks down as follows for a 15-piece order: the raw PCB costs 22.1USD, the electronic components 25.53USD, the motor 14.99USD, and the battery 6.49USD. (Note that the price of 3D printed parts is negligible as they total 2.24g of material, and that the module price will drop with bulk ordering.)

The crank and slider mechanism dominates the module design, volume, weight, and cost. It works by rotating a custom worm gear with two opposite thread angles, which is translated to linear motion through two gear racks that attach to raise or lower the appendages. To support this mechanism we chose a commercially available, affordable, strong, small, and light weight motor; specifically the 700:1 Sub-Micro Plastic Planetary Gearmotor (6mm diameter, 21mm length, 1.3g) from Pololu.

Beyond the off-the-shelf motor and the battery, modules consist almost entirely of FR4 and polyimide material, commonly known as rigid and flexible printed circuit boards (PCBs). We order these pre-soldered by Sandnwave for ease; because these fabrication houses are located in China, we also circumvent long lead times due to the ongoing shipping crisis. Beyond the PCBs, the module consists of a 3D printed bearing and motor holder which are snap-fit into holes in the PCB. We use the Formlabs 2.0 and the Carbon 3D printers, with Tough1500 and UMA90 material respectively, to produce the bearing, motor holder, and worm gear. While the resolution of the prints are important, the material itself only affects how quickly the parts wear down.

Fig.2 shows the breakdown of the mechanical parts as well as the top and side view of a robot. On the PCB top, it mounts the worm gear and motor pair, the bearing and motor holder, as well as the left and right sliders. The bearing and

Table 1. Examples of self-re-configurable modular and swarm robotic platforms, characterized in terms of properties related to scalable fabrication and operation.

Platform	Form factor[mm]	Weight[g]	Cost[USD]	Assembly time[min]
Jasmine robots[20]	$\sim 30 \times 30 \times 30$	-	130	-
Donuts[9]	46(diameter),70(tall)	25.4	587	48
Kilobots[21]	33(diameter),40(tall)	-	14*	15
Smarticles 1.0[2]	$151 \times 53 \times 25$	-	40.8*	-
<i>Smarticles 2.0</i>	$2000 \times 20 \times 17$	20	71	15

-no information *parts cost only

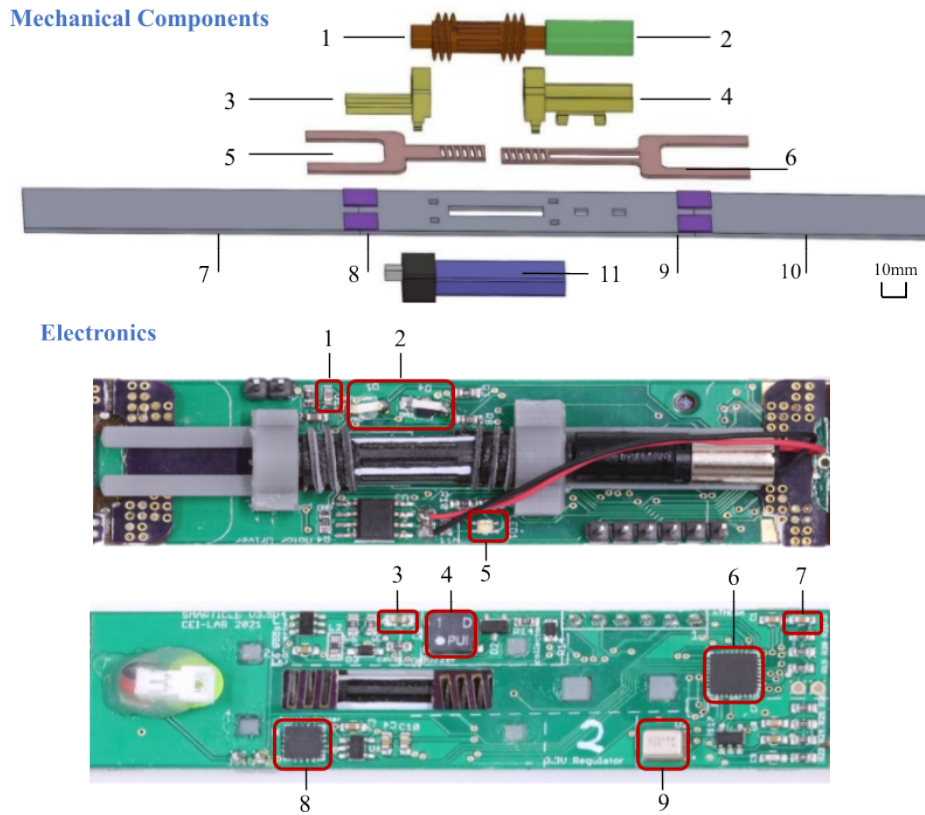


Fig. 2. Component overview. **Mechanical Components:** 1. Worm gear; 2. Planetary DC motor; 3. Motor bearing; 4. Motor holder; 5. Left slider; 6. Right slider; 7. Left appendage; 8. Flexible PCB link; 9. Center body; 10. Right appendage; 11. Battery. **Electronics:** 1. Light sensor; 2. IR encoders; 3. Motor current sensor; 4. Buzzer; 5. RGB LED; 6. Atmega328pb microcontroller; 7. Battery state sensor; 8. Accelerometer; 9. Microphone.

motor holder not only secures the worm gear and motor during the operation, but also help to guide the sliding motion of the gear racks. These parts are fitted on the center body, connected to the left and right appendage by 4 flexible PCB link pieces. The battery is mounted on the back of the module.

Each module is controlled by an 8-bit ATmega328pb microprocessor, making it compatible with the popular do-it-yourself (DIY) Arduino IDE programming framework. Modules have six sensing modalities. In terms of proprioception, they can measure their battery state, appendage load (motor current), appendage position through IR encoders, and orientation through a 3-axis accelerometer. In terms of exteroception, they can measure ambient light using an IR sensor, audio using a buzzer-microphone pair, and vibrations using the accelerometer. These sensing modalities compliment each other: acoustic signals can penetrate an entangled collective, light can address only perimeter modules, and, because

the robots are typically loosely entangled, mechanical vibrations translate only between neighboring modules.

To lower maintenance, the battery is connected to a coil embedded in the left appendage, such that the modules can be charged by loose placement on a wireless charger (Fig.1.B). The current charging circuit cost 85USD and simultaneously charges 5 robots fully over 6hrs. We have yet to optimize for cost and ease of use, i.e. the amount of misalignment the charger can handle for easier placement.

4 Fabrication

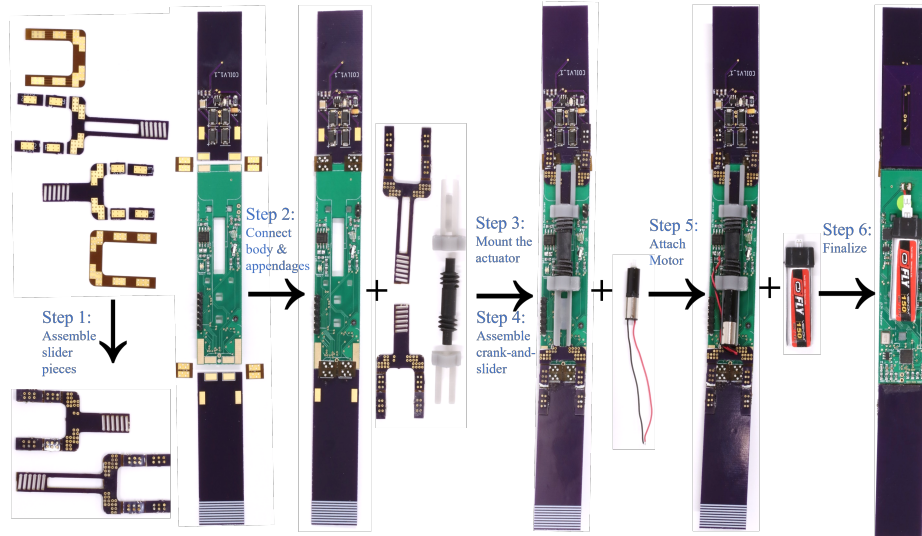


Fig. 3. Smarticle 2.0 assembly steps.

Fabrication time and ease are both critical to support user-adoption of swarm modular robot platforms. All electronic components can be mounted on the rigid PCB either in- or out of house. The latter requires less in-house expertise and labor, and is in fact economically advantageous due to the current shipping crisis. Excluding component soldering and 3D printing of components, the in-house assembly takes less than 15 minutes per robot and requires little prior knowledge on soldering techniques. The fabrication process involves six main steps (Fig. 3):

1. **Assemble slider pieces:** To support accurate, rapid, and inexpensive assembly of the flexible and rigid PCBs that make up the sliders, we added solder pads such that they can be laminated together in a re-flow oven. This process enable the pieces to self-align due to the surface tension created by the solder paste. Depending on the size of the oven, a few dozen sliders can be

produced in each batch. Alternatively, this step can be done with a carefully pointed heat gun.

2. **Connect body and appendages:** We connect the two appendages and the center body by soldering the four flexible link pieces on to each side. To assist in the alignment of PCBs, we perform this step on a 3D printed holder.
3. **Mount the actuator:** We snap-fit the bearing and motor holder to the center body PCB, to hold together the two sliders and the worm gear.
4. **Assemble crank-and-slider:** We solder the sliders to the appendages.
5. **Attach Motor:** We glue the motor into the motor holder and solder the motor connections onto the center body PCB.
6. **Finalize:** We plug in the battery and apply a thin layer of liquid electrical insulation paint on the surface of robot.

5 Characterization

In this section we characterize essential properties of the Smarticle 2.0 modules, including their actuation profile (accuracy/longevity, lifting strength, and holding strength) and sensor specifications (acoustic, orientation).

First, to test the repeatability and durability of the mechanical components, a module was programmed to raise-, pause-, lower-, and pause the appendages open-loop for 2s-3s-2s-3s, respectively. We repeated this behavior for 67min continuously, amounting to more than 400 cycles. We found that even without sensor feedback, the appendage motion is fairly symmetrical and accurate within a standard deviation of less than 2° , and persists over many cycles. Specifically, the left and right appendage minimum angle was found to $30.2 \pm 1.0^\circ$ and $35.8 \pm 1.2^\circ$ respectively; and the left and right appendage maximum angle was found to $88.0 \pm 0.9^\circ$ and $85.4 \pm 2.0^\circ$ respectively.

Second, we analyzed the appendage lifting force, by combining the governing equations for the crank and slider mechanism [22] and the worm gear force translation [23]. These parameters are also shown in Fig. 4.A. Geometrically, the distance from the end of the connecting rod to the crank axle, x , and the angle between the slider and the connecting rod, β , can be calculated as follows:

$$x = r\cos(\alpha) + \sqrt{l^2 - r^2\sin^2(\alpha)} \quad (1)$$

$$\beta = \cos^{-1}\left(\frac{x + r\cos(\pi - \alpha)}{l}\right) \quad (2)$$

where α is the angle of the crank, r is the rotating crank length, and l is the length of the connecting rod. The torque from the crank and slider on the appendage, τ , depends on F , the linear force pulling on the slider:

$$\tau = Fr\sin(\alpha + \beta) \quad (3)$$

Conversely, the motor stall torque, τ_{stall} , relates to the maximum linear force the crank and slider mechanism is capable of delivering, estimated as:

$$F = \frac{2\tau_{stall}}{d_{mean}} \left(\frac{\pi d_{mean} - fpsec(\zeta)}{p + \pi fd_{mean}sec(\zeta)} \right) \quad (4)$$

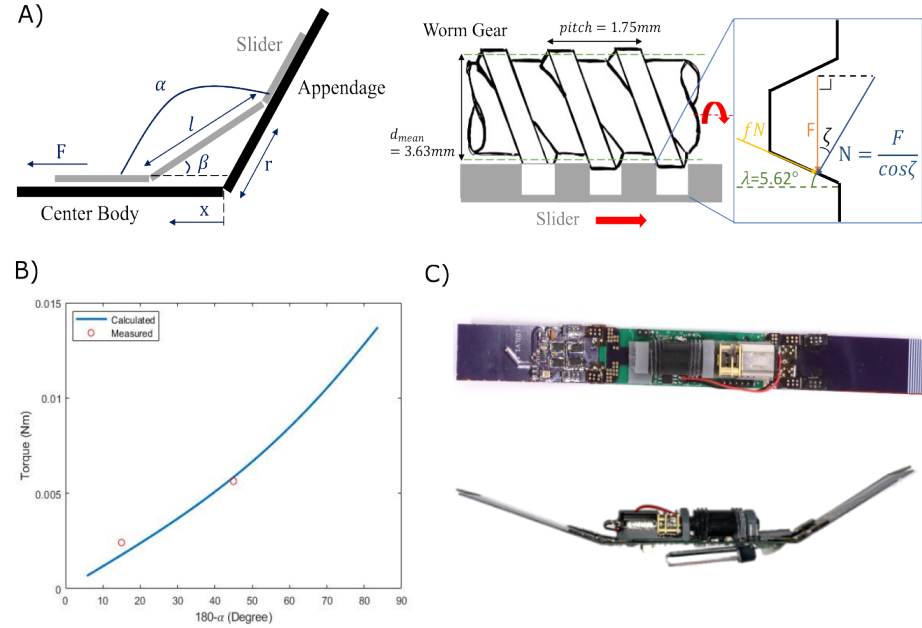


Fig. 4. A) Left: Kinematic forces acting on the worm gear; Right: Single-appendage view of the crank and slider mechanism, with design parameters. B) Lifting force of a single appendage. The blue line is the theoretical prediction, red data points show experimentally obtained values. C) Alternative design with a stronger motor.

where d_{mean} and p is the mean thread diameter and pitch of the worm gear, and ζ and f are the angle and amplitude of the normal force between the teeth and the grooves in the (FR4-based) rack, respectively. We now combine Eqs. 4 and 3 and iterate over all appendage angles to estimate their lifting force (Fig. 4.B). Note that the model is inaccurate due largely to the loss of efficiency in the worm-rack transmission and friction between the sliders and center body PCBs. We partially make up for this inaccuracy by tuning the value of f to two sets of real data points at low and high appendage angles gathered from the real modules. We see that the mechanism is strongest (can lift the highest load) when the appendage is near vertical, and vice versa. Practically, this means that when the appendage is at a 90° angle, the appendage can lift 3.42 modules placed 40mm out from the center body PCB; at 45° it can lift 1.7 modules; and at 10° it can lift 0.33 modules.

The real strength of the chosen mechanism is that it is non-back-drivable. This feature allow robots to maintain a joint angle without energy consumption, independent of load size (provided that it does not exceed the breaking point). As a rule of thumb, this property holds for worm gears with a lead angle smaller than $\text{atan}(\mu)$, where μ is the coefficient of friction. Estimating that μ is comparable

to two glass plates sliding against each other (0.4), we get that the lead angle, λ must be smaller than 21° - well beyond the 5.6° of our design. Practically, this means that the module's holding force is only limited by the bonding strength of the solder joints that attach the appendages to the main PCB. In other words, once in position, the module can hold a significant amount of weight without necessitating continuous power. In the spirit of keeping our robots intact, we have yet to perform destructive testing, but in preliminary tests we have loaded appendages with over 15 modules without mechanical failure.

The Smarticle 2.0 design is also compatible with other off-the-shelf motors such as the Micro Metal Gearmotors (cross section 10×12 mm) from Pololu. Taking a Pololu micro motor with gear ratio 298:1 (stall torque 20 OzIn) as an example, it uses the same PCB design only and takes some adjustment on the 3D printed parts to fit the motor as shown in Fig. 4.C. Assembling a Smarticle 2.0 with this motor follows the same steps as the Plastic Planetary Gearmotor design and takes similar assembly time. The overall weight of a Smarticle 2.0 is 25 grams and its total cost is slightly higher at 72.47USD. With this motor, when the appendage is at a 90° angle, the appendage can lift 41.6 modules placed 40mm out from the center body PCB; and at 10° angle, it can lift 2.04 modules. We will explore the functionalities of a heterogeneous collectives in the future.

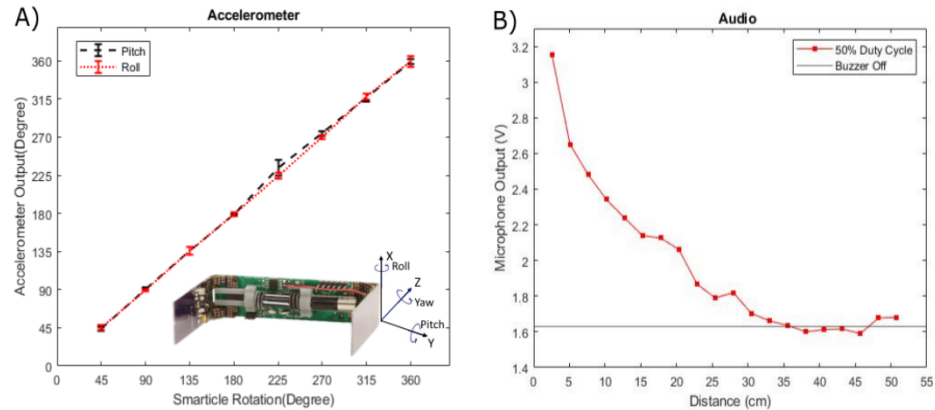


Fig. 5. A) Characterization of accelerometer accuracy: mean and standard deviation of ten measurements at each rotation. B) Microphone-buzzer detection between two modules.

Finally, Fig. 5.A-B shows a characterization of the onboard accelerometer and buzzer-microphone pair. We see that rotation around the accelerometer x-axis (roll) and y-axis (pitch), is accurately detected. We further see that at 50% power using the onboard microphone and buzzer pair, two modules can signal over 300mm range, equivalent to 1.5 the module body length. This value can be tuned by adjusting the average buzzer power (the pulse width) of the carrier signal.

6 Multi-Robot Demonstrations

While this paper is focused mainly on describing the design of and characterizing individual modules, there are many avenues for extension of this work. In this section, we show exploratory multi-robot experiments to illustrate the platform's potential to support both active matter and robotic functionality in the future.

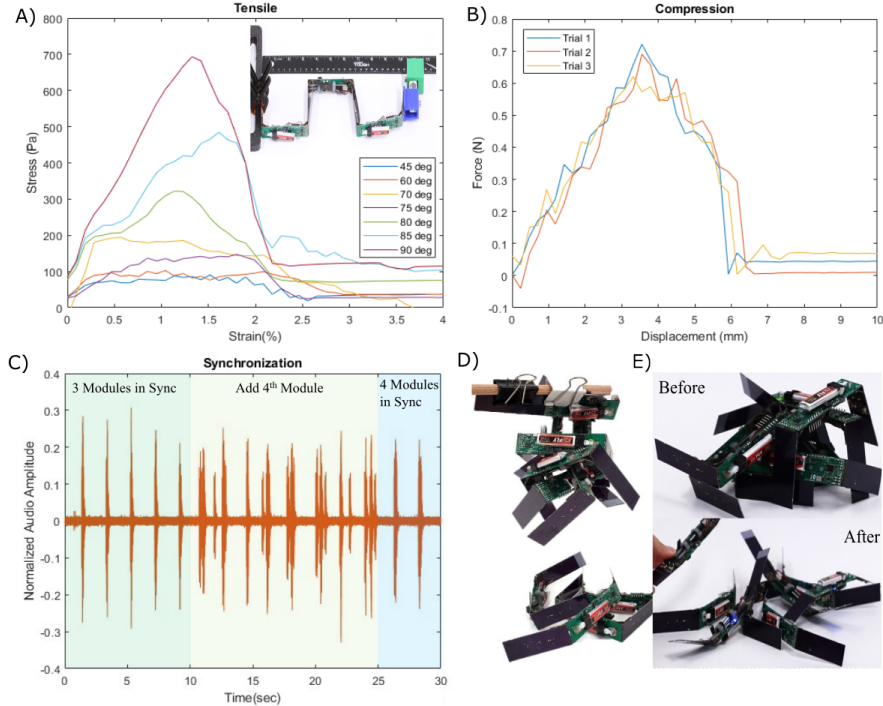


Fig. 6. A) Three-module tensile test at different appendage angles. B) Three-module compression tests with appendages located at 90° . C) Recorded audio signal of acoustic synchronization tests. 0-10s shows the beeps from three synchronized modules; at 10s an unsynchronized module is added to the collective; past 25s all four modules have synchronized again. D) Active entanglement by hanging multiple modules. E) Before and after of disassembly test with 7 modules.

The Smarticle 2.0 platform can be used for both taskable robot- and smart matter experiments. As a simple demonstration of this concept, Fig. 6.A-B shows tensile and compression tests of 3 modules arranged in a 2D chain. Note that to calculate stress in Fig. 6.A, we assume that the cross-sectional area of the "Smarticle 2.0 material" remains constant; i.e. only the force changes. The experiment shows how the material, similar to most hyperelastic polymers, first exhibits a roughly linear profile due to linkage deflection, then rapidly declines in stress because the modules start to slide against each other. As one would

expect, sliding occurs earlier with lower appendage angles; i.e. the higher the appendage angle, the higher the elastic modulus.

The compression test was limited to Smarticles with 90° appendages, because at lower angles, the center module would immediately start sliding. In the three repeated trials, we again see a roughly linear profile caused by link deflection, and then a rapid decline in compression strength due to module sliding.

To demonstrate that, mechanically, the Smarticle 2.0 modules have a form factor and weight that permits entanglement, we attached a single module to a ruler and manually hung as many other modules off it as possible (Fig. 6.D). In five repeated trials, we achieved 7, 8, 9, 8, and 9 modules. In the near future, we plan to repeat this experiment with active entanglement - i.e. by placing modules in a bin, having them actively entangle, and then pulling out globs of "Smarticle 2.0 material" with a stick similar to past papers demonstrating entanglement of passive staples [19], fire ants, and worm blobs [24].

Finally, to demonstrate that material composed of entangled Smarticle 2.0 modules can actively undergo a phase change, we manually assembled a glob of 7 modules with appendages at 90°, and programmed them to unfold upon hearing an acoustic signal in close proximity(Fig. 6.E). In doing so, the glob went from a volume of 1853.8cm³ to 3745.4cm³, i.e. an order of magnitude change, similar to a phase change from solid to liquid.

As a building block for more complex and distributed coordination schemes, we demonstrated acoustic synchronization of four modules using the Kuramoto model [25]. In Fig. 6.C, we show how this works, by placing a non-synchronized module next to three previously synchronized modules, while recording their buzzes with a separate module. In this case the modules synchronized over 9 cycles. In longer experiments where all four modules started unsynchronized, full synchronization took 17 cycles. These characteristics can be optimized with better coupling factors, but the general concept of module synchronization is promising for future work on consensus and collective motions.

In Fig. 7.A, we demonstrate how the onboard accelerometer can be used for tactile communication; i.e. by sensing changes in orientation. We manually poke a module, causing it to activate by flapping its appendages, which causes the signal to propagate to other nearby robots. It is worth noting that the signal amplitude is heavily dependent on where along the center body PCB the modules connect, and that the flapping action can cause unwanted accelerometer readouts that self-activate the module. In Fig. 7.B we included a small inhibitory period, thereby avoiding self-activation and only flapping the appendages once upon external stimulus.

7 Summary

We presented and characterized a design optimized for scalable fabrication and operation of robotic modules, capable of 3D entanglement by a range of scientific users. This relatively new subfield of 3D entangled robots presents unique opportunities related to active matter and taskable modular robots as evidenced by entangled social organisms in nature, but also unique research challenges related

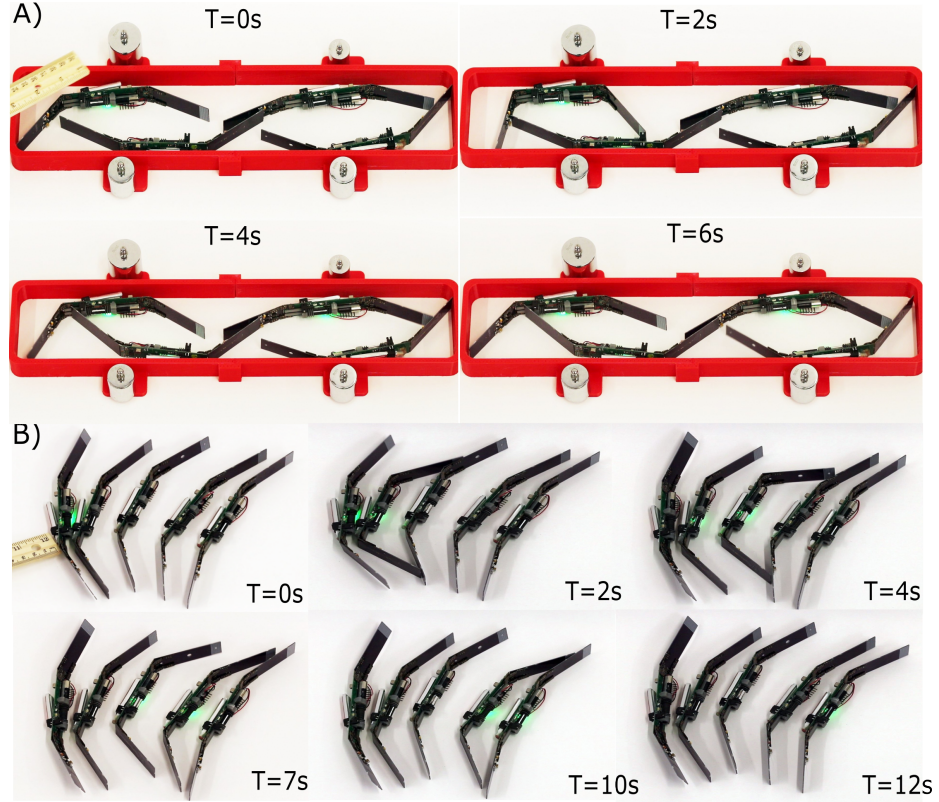


Fig. 7. A-B) Smarticles sequentially activate each other through tactile cues.

to communication and consensus algorithms, reconfiguration, and mobility. In future work, we aim to scale up the size of our collective and demonstrate more complex multi-agent behaviors in both hardware and simulation. The design files for these robots are available upon request from the authors.

Acknowledgements

This project was funded by NSF awards #1933284 and #2042411, and the Packard Fellowship for Science and Engineering. The authors would like to acknowledge many fruitful discussions with Prof. Goldman at the Georgia Institute of Technology.

References

1. S. C. Goldstein, J. D. Campbell, and T. C. Mowry, “Programmable matter,” *Computer*, vol. 38, no. 6, pp. 99–101, 2005.

2. W. Savoie, A. Pazouki, D. Negrut, and D. Goldman, “Smarticles: design and construction of smart particles to aid discovery of principles of smart, active granular matter,” in *The First International Symposium on Swarm Behavior and Bio-Inspired Robotics*, 2015.
3. P. Chvykov, T. A. Berrueta, A. Vardhan, W. Savoie, A. Samland, T. D. Murphrey, K. Wiesenfeld, D. I. Goldman, and J. L. England, “Low rattling: A predictive principle for self-organization in active collectives,” *Science*, vol. 371, no. 6524, pp. 90–95, 2021.
4. G. Gardi, S. Ceron, W. Wang, K. Petersen, and M. Sitti, “Microrobot collectives with reconfigurable morphologies, behaviors, and functions,” *Nature communications*, vol. 13, no. 1, pp. 1–14, 2022.
5. J. Daudelin, G. Jing, T. Tosun, M. Yim, H. Kress-Gazit, and M. Campbell, “An integrated system for perception-driven autonomy with modular robots,” *Science Robotics*, vol. 3, no. 23, 2018.
6. K. Gilpin and D. Rus, “Modular robot systems,” *IEEE robotics & automation magazine*, vol. 17, no. 3, pp. 38–55, 2010.
7. B. Haghhighat, E. Droz, and A. Martinoli, “Lily: A miniature floating robotic platform for programmable stochastic self-assembly,” in *2015 IEEE International Conference on Robotics and Automation (ICRA)*. IEEE, 2015, pp. 1941–1948.
8. S. Ceron, M. A. Kimmel, A. Nilles, and K. Petersen, “Soft robotic oscillators with strain-based coordination,” *IEEE Robotics and Automation Letters*, vol. 6, no. 4, pp. 7557–7563, 2021.
9. N. J. Wilson, S. Ceron, L. Horowitz, and K. Petersen, “Scalable and robust fabrication, operation, and control of compliant modular robots,” *Frontiers in Robotics and AI*, vol. 7, p. 44, 2020.
10. S. Li, R. Batra, D. Brown, H.-D. Chang, N. Ranganathan, C. Hoberman, D. Rus, and H. Lipson, “Particle robotics based on statistical mechanics of loosely coupled components,” *Nature*, vol. 567, no. 7748, pp. 361–365, 2019.
11. R. Warkentin, W. Savoie, and D. I. Goldman, “Locomoting robots composed of immobile robots,” in *2018 Second IEEE International Conference on Robotic Computing (IRC)*. IEEE, 2018, pp. 224–227.
12. W. Savoie, T. A. Berrueta, Z. Jackson, A. Pervan, R. Warkentin, S. Li, T. D. Murphrey, K. Wiesenfeld, and D. I. Goldman, “A robot made of robots: Emergent transport and control of a smarticle ensemble,” *Science Robotics*, vol. 4, no. 34, 2019.
13. A. Nilles, S. Ceron, N. Napp, and K. Petersen, “Strain-based consensus in soft, inflatable robots,” in *2022 IEEE 5th International Conference on Soft Robotics (RoboSoft)*. IEEE, 2022, pp. 789–794.
14. K. Gilpin, A. Knaian, and D. Rus, “Robot pebbles: One centimeter modules for programmable matter through self-disassembly,” in *2010 IEEE International Conference on Robotics and Automation*. IEEE, 2010, pp. 2485–2492.
15. P. Swissler and M. Rubenstein, “Fireant3d: a 3d self-climbing robot towards non-latticed robotic self-assembly,” in *2020 IEEE/RSJ International Conference on Intelligent Robots and Systems (IROS)*. IEEE, 2020, pp. 3340–3347.
16. W. Savoie, S. Cannon, J. J. Daymude, R. Warkentin, S. Li, A. W. Richa, D. Randall, and D. I. Goldman, “Phototactic supersmarticles,” *Artificial Life and Robotics*, vol. 23, no. 4, pp. 459–468, 2018.
17. W. Zhou and N. Gravish, “Density dependent synchronization in contact-coupled oscillators,” *arXiv preprint arXiv:2012.07124*, 2020.

18. Y. Ozkan-Aydin, D. I. Goldman, and M. S. Bhamla, “Collective dynamics in entangled worm and robot blobs,” *Proceedings of the National Academy of Sciences*, vol. 118, no. 6, 2021.
19. N. Gravish, S. V. Franklin, D. L. Hu, and D. I. Goldman, “Entangled granular media,” *Physical review letters*, vol. 108, no. 20, p. 208001, 2012.
20. H. Woern, M. Szymanski, and J. Seyfried, “The i-swarm project,” in *ROMAN 2006-The 15th IEEE International Symposium on Robot and Human Interactive Communication*. IEEE, 2006, pp. 492–496.
21. M. Rubenstein, C. Ahler, and R. Nagpal, “Kilobot: A low cost scalable robot system for collective behaviors,” in *2012 IEEE international conference on robotics and automation*. IEEE, 2012, pp. 3293–3298.
22. R. Hartenberg and J. Danavit, *Kinematic synthesis of linkages*. New York: McGraw-Hill, 1964.
23. R. Budynas and K. Nisbett, *EBOOK Shigley’s Mechanical Engineering Design 11e in SI Units*. McGraw-Hill Education (Asia), 2020.
24. D. Hu, S. Phonekeo, E. Altshuler, and F. Brochard-Wyart, “Entangled active matter: From cells to ants,” *The European Physical Journal Special Topics*, vol. 225, no. 4, pp. 629–649, 2016.
25. J. A. Acebrón, L. L. Bonilla, C. J. P. Vicente, F. Ritort, and R. Spigler, “The kuramoto model: A simple paradigm for synchronization phenomena,” *Reviews of modern physics*, vol. 77, no. 1, p. 137, 2005.